Int. J. Nano Dimens., 8 (3): 216-223, Summer 2017

ORIGINAL ARTICLE

# Investigations on the structural, electrical properties and conduction mechanism of CuO nanoflakes

*Muthurani Shunmugam[1]; Hirankurmar Gurusamy[2]; Prem Anand Devarajan[1]**

*[1]Department of Physics, St. Xavier's College, Tirunelveli, Tamilnadu, India*
*[2]Centre for Scientific and Applied Research, PSN College of Engineering and Technology, Tirunelveli, India*

Received 27 February 2017; revised 06 May 2017; accepted 15 May 2017; available online 22 May 2017

**Abstract**

Copper oxide (CuO) nanostructures are of particular interest because of their interesting properties and promising applications in batteries, super capacitors, solar cells, gas sensors, bio sensors, nano fluids and catalysis. In Recent past, more efforts have been received to design materials with different properties which is dependent on morphology. In this work cupric oxide nano flakes were prepared by surfactant assistant wet chemical method. Samples were synthesized using ethylene glycol as the surfactant and by changing the concentration of ethylene glycol by 0 M, 0.05 M, 0.1 M, and 0.2 M. X-Ray diffraction (XRD) analysis confirmed the crystalline nature of as synthesized materials. Crystallite size and crystallographic parameters were calculated. Flakes like morphology of materials were elucidated by Scanning Electron Microscope (SEM). Using Electrochemical Impedance spectroscopy, variation of real and imaginary part of impedance, electrical conductivity with frequency and temperature were also studied. It was observed that sample with 0.1 M surfactant has high conductivity when compared to other samples. It was noted that the particle size and electrical properties of Copper oxide nano flakes were affected by concentration of the surfactant. The Conduction mechanism of Copper oxide is discussed on the basis of Correlated Barrier Hopping (CBH) model.

**Keywords**: *CBH model; Cupric oxide; Ethylene glycol; Impedance spectroscopy; Nano flakes.*

**How to cite this article**

*Muthurani S, Hirankumar G, Prem Anand D. Investigations on the structural, electrical properties and conduction mechanism of CuO nanoflakes. Int. J. Nano Dimens., 2017; 8 (3): 216-223.*

## INTRODUCTION

Nano metal oxide semiconductors draws attention because of their unique physicochemical properties than bulk materials. The uniqueness of Copper oxide is its monoclinic unit cell and square planar co-ordination of copper with oxygen. All the other metal monoxides like MnO, FeO, CoO and NiO have cubic rock salt structure and octahedral coordination [1]. Copper oxide has promising applications in Li–ion batteries [2], photo catalyst [3], super capacitors [4], gas sensors [5], nano fluids [6], arsenic removal [7] etc. As of now, greater attention has been received to synthesize materials with different morphology since efficiency of the materials change with their morphology. Xiadu et al [2] discussed the variation of electrochemical properties between Copper oxide architecture and Copper oxide nano plates. Qingwei et al [3] proved that dandelion shaped Copper oxide having 56% efficiency in degradation of Rhodamine B whereas octahedron shape has only 46% efficiency. A number of literatures discusses about synthesis of different morphology of Copper oxide like nano rods ,nano ribbons [8], nano plates [9], nanosheets [10], flower like [11] octahedran, sphere, strip, Dandellon [3], nanowires, nano belts [12] , nano cubes and leaf like [13] structures. Morphology can also be changed by changing pH, temperature, precursor materials, reaction conditions, preparation methods and surfactants. In the present case, effort is taken to change the morphology of Copper oxide, by changing the concentration of surfactant. Our aim is to investigate the effect of Ethylene glycol (EG) as surfactant on the structural and electrical properties of Copper oxide nanoflakes.

* Corresponding Author Email: *dpremanand@yahoo.co.in*

## EXPERIMENTAL

Cupric nitrate trihydrate [$Cu(NO_3)_2 \cdot 3H_2O$] (Himedia 99.5% purity), Ethylene glycol [$CH_2OH$ $CH_2OH$] (Nice chemicals 99%) and sodium hydroxide pellets [NaOH] (Nice chemicals) are the chemicals used in this experiment. They were analytical reagent grade and used without further purification. Cupric oxide was prepared by surfactant assistant wet chemical method. 0.1M of cupric nitrate solution and 0.2 M of NaOH solutions were made separately using deionized water. With the blue coloured cupric nitrate solution, ethylene glycol (EG) was added and allowed to stir for an hour. Freshly prepared sodium hydroxide solution was added drop by drop with continuous stirring until the solution pH reached to 11. Mean while blue precipitation was formed and it turned into black [14]. The precipitation was then washed several times by distilled water and ethanol using suction funnel. Washed samples were dried at room temperature for 24 hrs. Then it was kept in oven at 120° C for 10 hrs.

Following the above procedure four samples were synthesized using different concentrations of surfactant (ethylene glycol). 0 M, 0.05 M, 0.1M and 0.2 M Ethylene glycol was added such that the molarity of surfactant is lower, equal and higher than the molarity of precursor salt. Four samples are named as EG (0), EG (0.05), EG (0.1), EG (0.2).

The XRD pattern was recorded by XPERT-PRO diffractometer using Cu-Kα radiation (λ=1.54 Å) in order to confirm the crystalline nature and to determine the phase present in the prepared materials. SEM analysis was carried out using scanning electron microscope Carl Zeiss EVO 18 at 35 KX magnification. The as prepared samples were made into pellets using hydraulic pellet press applying 7 Tons of pressure for one minute. Impedance was measured using biologic SP -300 electrochemical workstation using stainless steel plates as electrodes. The measurement was taken in the frequency range from 1 Hz to 7 MHz and the temperature range from room temperature to 80°C.

## RESULTS AND DISCUSSIONS

*XRD analysis*

Fig. 1 shows the XRD pattern of the Copper oxide nano flakes. The formation of crystalline Copper oxide nano structures was confirmed by the XRD pattern. The crystallite sizes have been calculated for highest four peaks of all the samples using Debye–Scherrer's equation $D = \frac{K\lambda}{\beta \cos\theta}$ [15] Where K is constant (shape factor, about 0.89), λ is x-ray wavelength used (1.54 Å), β is full width at half maximum (FWHM). Average crystallite size calculated were 21, 23, 25 and 16 nm for EG (0), EG (0.05), EG (0.1) and EG (0.2) respectively. Particle size of the Samples using 0 M, 0.05 M and 0.1 M of surfactant is more or less same but Sample synthesized using highest concentration of surfactant yields smallest crystallite size. It shows that appropriate amount of surfactant only can reduce the particle size. It is observed that all the peaks in the XRD patterns are consistent with the JCPDS data (80-1916) of the Copper oxide. All the diffraction peaks can be indexed to the monoclinic phase of Copper oxide with lattice parameters a=4.6830 Å, b=3.428 Å, c=5.1290, β=99.42, space group Cc (9). No other impurity peaks were identified.

*SEM analysis*

Fig. 2 shows the SEM images of ((a) EG (0), (b) EG (0.05), (c) EG (0.1), (d) EG (0.2)) Copper oxide nano flakes. SEM images show all the samples have flakes like morphology. Addition of EG did not affect the morphology. This is may be due to the loss of structure directing properties of EG in the high alkaline (pH=11) solution [16]. But size affected by the surfactant is shown by Fig. 2(d) which shows small size flakes than other samples. Crystallite size calculated from XRD analysis also confirmed this.

*Impedance spectroscopy analysis*

Fig. 3 shows the variation of real part of impedance to imaginary part of impedance (Nyquist plot) for the samples (a) EG (0), (b) EG (0.05), (c) EG (0.1) and (d) EG (0.2). Fig. 3 reveals that Nyquist plot of all the samples show a depressed semicircle pattern without any spike, which follows the equivalent circuit of parallel combination of a resistance and a capacitance [17]. This itself indicates conductivity predominated by electrons than the ions. Nyquist plot inferred that impedance decreases with increase of temperature which shows the materials having the behavior of negative temperature coefficient of resistance (NTCR) like semiconductors [18]. Bulk resistances and the dc conductivity of the samples were extracted by fitting the Nyquist plot using z-fit software. DC conductivities of all the samples

at different temperatures have been tabulated in Table 1.

Table 1 infers that EG (0.2) which has smallest particle size has lowest electrical conductivity. EG (0.1) which has highest particle size has highest conductivity. It may be due to quantum confinement effect.

Fig. 4 shows the temperature and frequency dependent conductivity of the samples EG (0) and EG (0.1). The Figure indicates that the conductivity variation shows similar trend for all the temperature. It has two regions such that low frequency plateau region and high frequency dispersion region. In plateau region applied field frequency is lower than the hopping frequency (frequency at which change in slope of the pattern occurs is known as hopping frequency). At low frequency region, a conductance spectrum is almost independent of frequency. This is because the occurrence of random hopping of charge carriers. When the applied AC frequency higher than hopping frequency conductivity increase notably [19]. As the frequency increases the localized states also (defects) increase, which cause the increase of conductivity at higher frequency. This indicates Conductivity originates from hopping of charge carriers between two sites [20]. At high frequency, conductance spectra merge together and show temperature independent nature of conductivity.

Total conductivity due to hopping mechanism is governed by johnschrs power law [21]

$$\sigma_{total} = \sigma_{dc} + \sigma_{ac} = \sigma_{dc} + A\omega^{s} \quad (1)$$

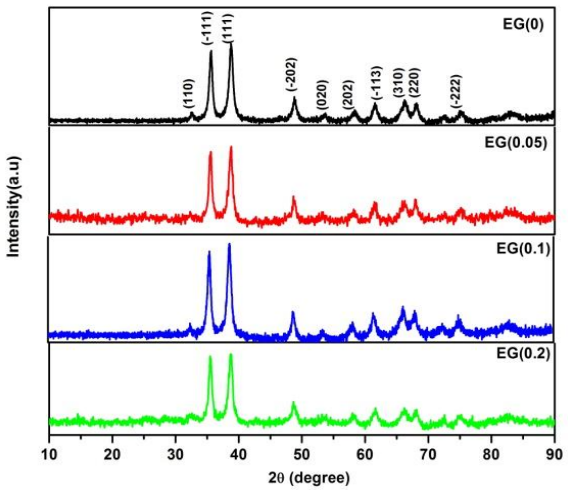


Fig. 1: XRD patterns of the CuO nano flakes EG (0), EG (0.05), EG (0.1), EG (0.2).

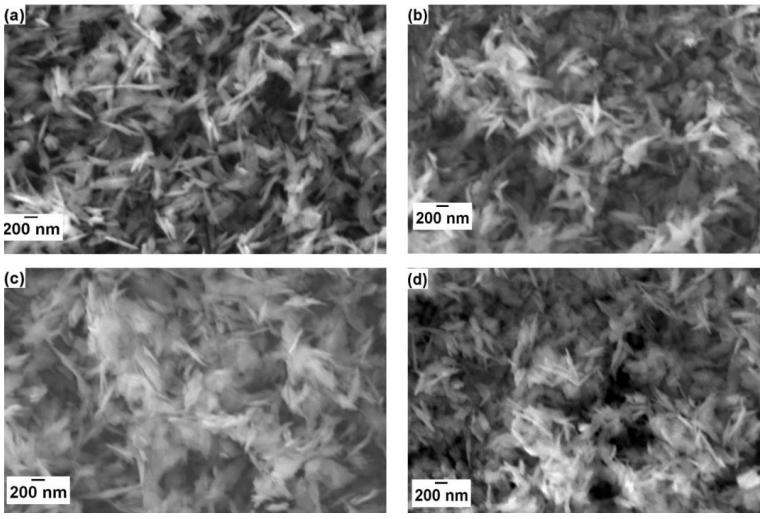


Fig. 2: SEM images of CuO nanoflakes (a) EG(0), (b) EG (0.05), (c) EG (0.1), (d) EG (0.2).

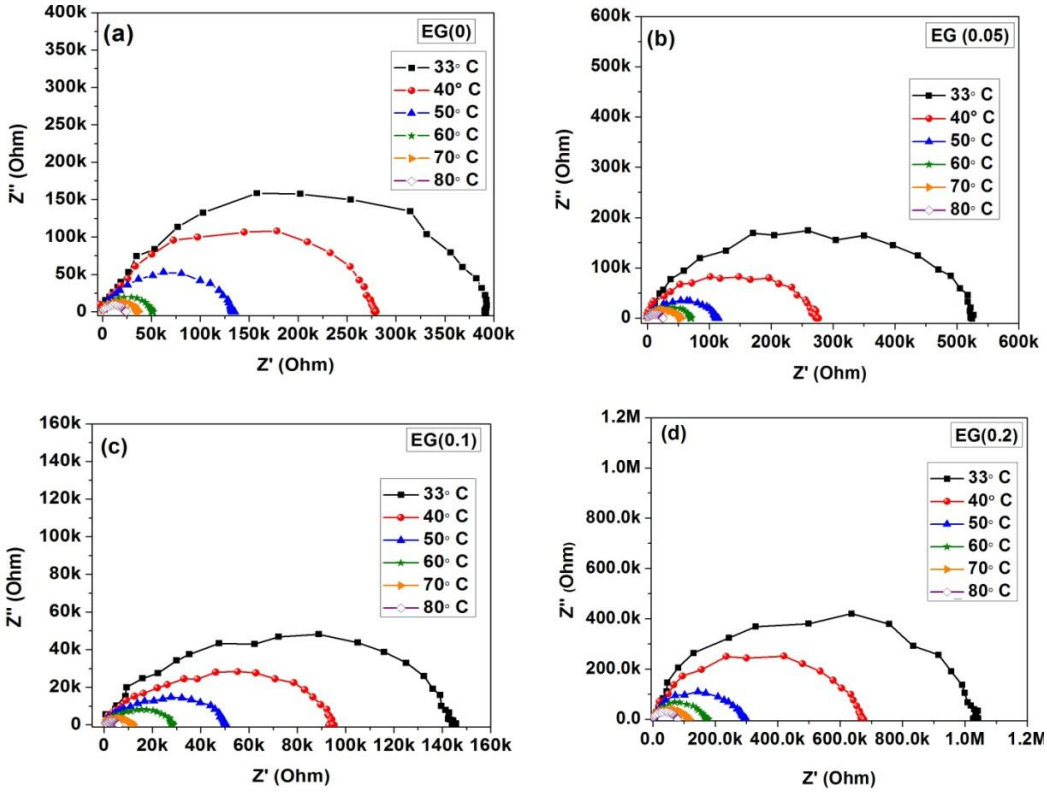


Fig. 3: Nyquist plot for CuO nano flakes (a) EG (0), (b) EG(0.05), (c) EG (0.1), (d) (EG (0.2).

Table 1: DC Conductivity of CuO nanoflakes EG(0), EG(0.05), EG (0.1), (EG (0.2) for various temperatures.

| Temperature in °C | Conductivity in S/Cm | | | |
|---|---|---|---|---|
| | EG(0) | EG (0.05) | EG(0.1) | EG(0.2) |
| 33 | 3.40 E-07 | 1.49 E-07 | 6.08E-07 | 0.937E-07 |
| 40 | 4.75E-07 | 2.82 E-07 | 9.23 E-07 | 1.44E-07 |
| 50 | 9.84 E-07 | 6.87 E-07 | 1.724E-06 | 3.27E-07 |
| 60 | 2.56 E-06 | 1.09E-06 | 3.10E-06 | 5.48E-07 |
| 70 | 3.65 E-06 | 1.43 E-06 | 7.70E-06 | 8.28E-07 |
| 80 | 5.52 E-06 | 3.07 E-06 | 1.52E-05 | 1.22E-06 |

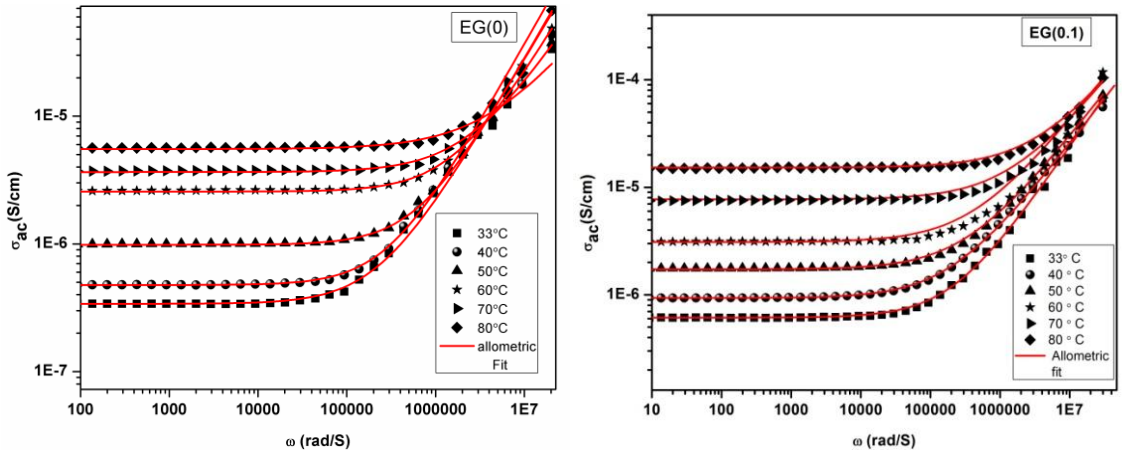


Fig. 4: Variation of a.c conductivity with frequency and for CuO nanoflakes EG (0) and EG (0.1).

A is temperature dependent constant. S is frequency exponent. The magnitude of S and its dependence of temperature tell about the conduction mechanism involved in the concerned material. To find the conduction mechanism involved in the present case, S value has been evaluated for various temperature by fitting equation 1to the experimental data of EG (0) and EG (0.1). In Fig. 4, symbol shows the experimental data of conductivity and the line indicates allometric fit of the data for the samples EG (0) and EG (0.1).

Fig. 5 shows the variation of S values with temperature which inferred that the frequency exponent values are dependent on temperature. This strongly suggests that conductivity mechanism follows the Correlated Barrier Hopping (CBH) model [22]. This model deals with hopping of carriers between two sites over a barrier rather than tunneling and the distance between two sites is considered as a barrier height [23]. In addition to the conduction mechanism model, S value also tells about the degree of order of the system. If S < 1, the system is said to be order one. Increasing value of S more than unity indicates the increase of disorder of the system [24]. In the present case S > 1 for EG (0) and S < 1 for EG (0.1) indicates that adding of 0.1M of EG increases the order of the system. This may be due to templating effect of EG (0.1). Fig. 6 shows Arrhenius plot i.e the variation of dc conductivity with temperature. Arrhenius plot depicts that the dc conductivity of the Copper oxide nano flakes increases with temperature which tells the electrical conduction in this process is thermally activated. The variation is linear with temperature and so obeying

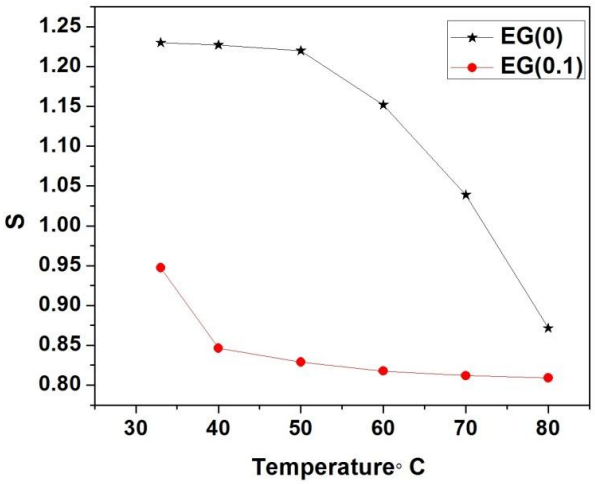


Fig.5: Variation of frequency exponent with temperature for CuO nanoflakes EG (0) and EG (0.1).

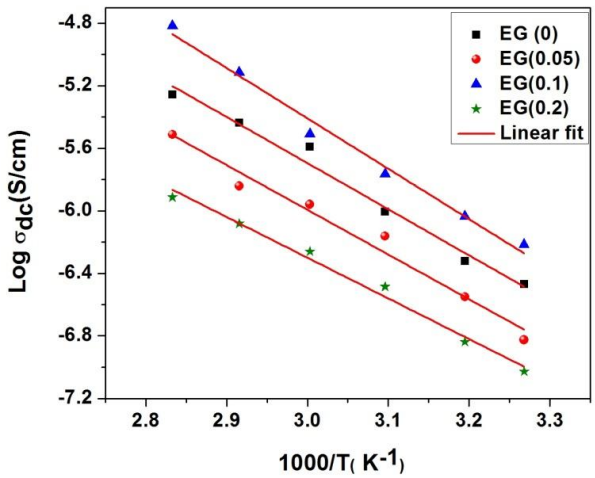


Fig. 6: Arrhenius plot of dc conductivity for CuO nanoleaves EG (0), EG(0.05), EG (0.1), (EG (0.2).

Arrhenius relation $\sigma_{dc} = \sigma_0 \exp\left(\frac{-E_a}{K_B T}\right)$ [24] where the symbols follow the usual meaning. The activation energy calculated for the samples were 0.59, 0.57, 0.63, 0.51 for EG (0), EG (0.05), EG (0.1), and EG (0.2) respectively.

Fig. 7 shows the variation of real part of impedance with temperature for (a) EG (0), (b) EG (0.05), (c) EG (0.1) and (d) EG (0.2). For all the samples the variation of Z′ follow the similar pattern. Z′ value decreases with increasing frequency and temperature. At high frequency Z′ values merge together and show temperature independent nature. This is due to release of space charge as a result of reduction of the barrier properties of the materials with rising of temperature [25]. The change over frequency (at which the spectra changes it state from frequency independent nature to frequency dependent nature) is increased with increase of temperature.

Fig. 8(a and b) shows the variation of Z″ with frequency of all the samples at room temperature and 80°C respectively. Fig. 8(c and d) shows the variation of Z″ with frequency at various temperature for the samples EG (0) and EG(0.1) respectively. The variation of Z″ with frequency showed a peak with characteristic frequency maxima ($\omega_{max}$) which depends on temperature. So that the relaxation presents in the Copper oxide nano flakes is a temperature dependent relaxation. The peaks appear when the hopping frequency of localized charge carriers becomes approximately equal to the applied electric field frequency.

In Fig. 8(c and d), the peak position of Z″ shifts towards higher frequency side as the temperature increases. Because hopping frequency of charge carriers increase with temperature. Relaxation time (τ) was calculated for sample EG (0) and EG (0.1) using the relation $\omega_{max}\,\tau = 1$ was obtained by fitting Z″ vs log ω plot using Lorentian fit. The magnitude of Z″ at $\omega_{max}$ decreases with the temperature indicating the presence of space charge polarization at low frequency which disappears at high frequency [26]. It is observed that relaxation time found from Z″ peak decreases with increase in temperature and it follows the Arrhenius relation.

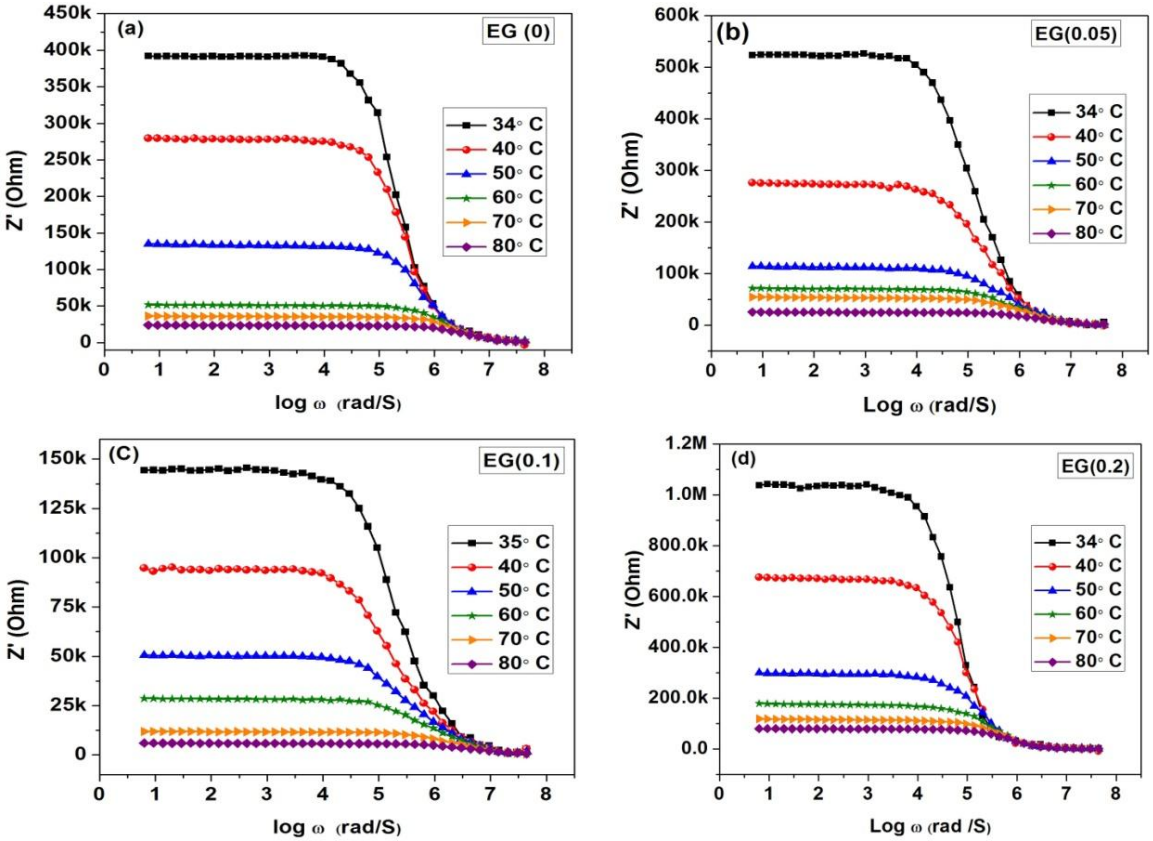


Fig. 7: Plot of real part of impedance vs frequency for(a) EG (0),(b) EG (0.05), (c)EG (0.1), (d)EG (0.2).

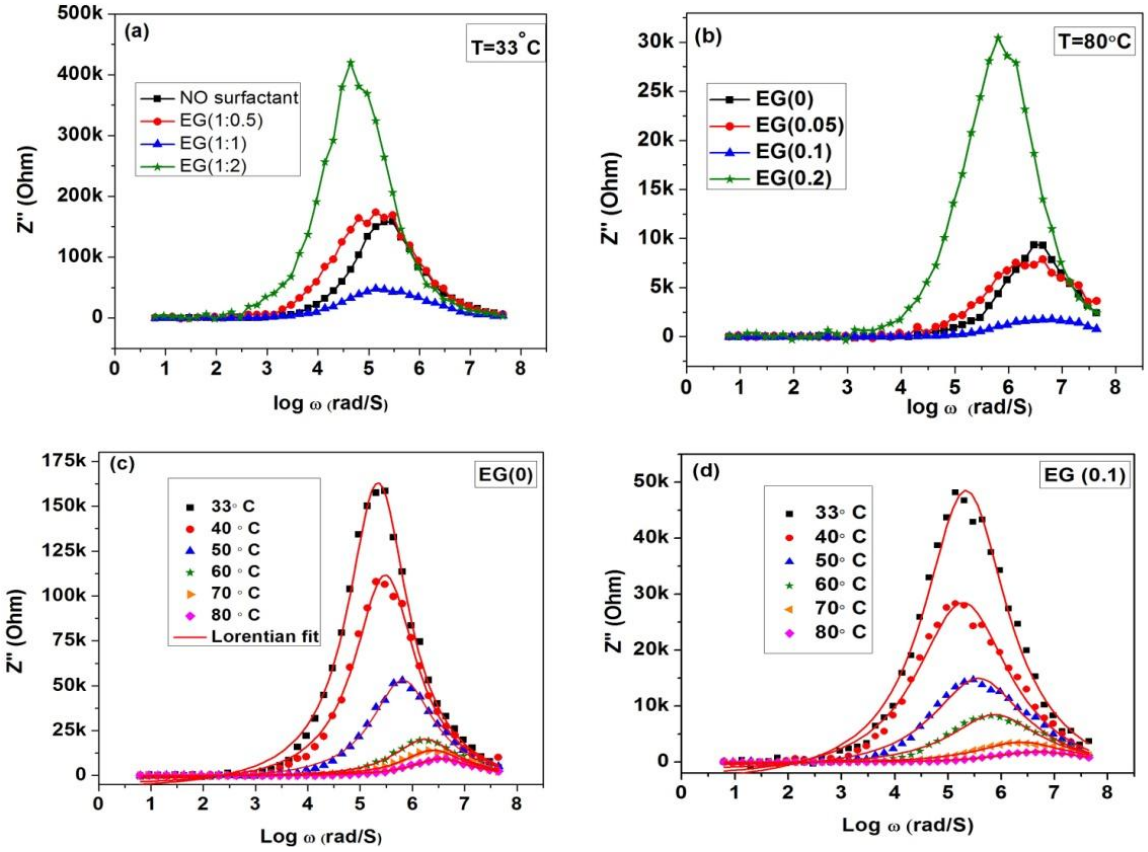


Fig. 8: Plot of imaginary part of impedance with frequency for all samples at (a) 33°C (b) 80°C and at all temperatures for (c) EG (0) and (d) EG (0.1).

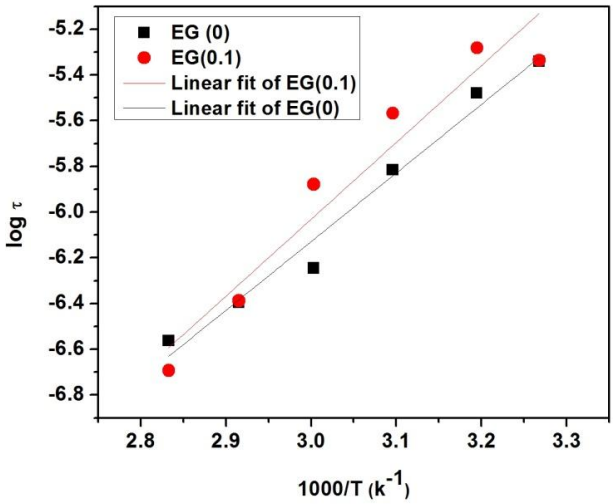


Fig. 9: Arrhenius plot of relaxation time for CuO nano flakes EG (0) and EG (0.1).

Fig. 9 shows the Arrhenius relation between log ( and 1000/T for EG (0) and EG (0.1). Activation energies calculated from the Arrhenius plot was 0.59 and 0.67 for EG (0) and EG (0.1) respectively within the fitting error. These values are matched to the activation energy calculated from dc conductivity, reveals that thermal energy given to the material is used for hopping of charge carriers only.

## CONCLUSIONS

Copper oxide nano flakes have been prepared using simple wet chemical method using ethylene glycol as surfactant with three different concentrations. XRD results confirmed the crystalline nature of the materials and monoclinic structure of copper oxide. Crystallite sizes calculated were 21, 23, 25 and 16 nm for EG(0), EG(0.05), EG(0.1) and EG(0.2) respectively. Higher ratio of EG only reduces the particle size for the present experimental conditions. SEM images elucidated the nano flakes morphology of synthesized cupric oxide materials. Structural and electrical properties of the materials met effective changes due to the change of the concentration of Ethylene glycol have been discussed. Impedance studies showed that, Copper oxide which was prepared by adding equal molarity of ethylene glycol with the cupric nitrate (EG (0.1)) enhances the electrical conductivity properties . Conduction mechanism of the Copper oxide nano flakes has been discussed.

## CONFLICT OF INTEREST

The authors declare that there is no conflict of interests regarding the publication of this manuscript.

## REFERENCES


[1] Kibriya S., Bhabesh K., Nath K. S., (2013), Study of structural and dielectric properties of copper oxide nanoparticles prepared by wet chemical precipitation method. *Int. J. Nanosci.* 12: 13500361 - 13500365.

[2] Xiaodi L., Guangyin L., Lijuan W., Yinping L., Yupei M., Jianmin M., (2016), Morphology and facet-controlled synthesis of Copper oxide micro/nanomaterials and analysis of their lithium ion storage properties. *J. Power Sources.* 312: 199-206.

[3] Qingwei Z., Yihe Zh., Jiajun W., Fengshan Zh., Paul K., Chu A, (2011), Microwave synthesis of cuprous oxide micro-/nanocrystals with different morphologies and photocatalytic Activities. *J. Mater. Sci. Technol.* 27: 289-295.

[4] Baiju V., Izan I. M., Jamil I., Mashitah M., Yusoff, R. J., (2015), High performance asymmetric supercapacitors using electrospun copper oxide nanowires anode. *J. Alloys. Compd.* 633: 22-30.

[5] Ming Q. E., (2011), Copper oxide nanoparticle sensors for hydrogen cyanide detection unprecedented selectivity and sensitivity. *Sens. Actuators. B.* 155: 692-698.

[6] Kiyuel K., Chongyoup K.,(2005), Viscosity and thermal conductivity of copper oxide nanofluid dispersed in ethylene glycol. *Korea-Aust. Rheol. J.* 17: 35-40.

[7] ] Reddy K. J., McDonald K. J., King H., (2013), A novel arsenic removal process for water using cupric oxide nanoparticles. *J. Colloid Interface Sci.* 397: 96-102.

[8] Yu Ch., Hua Ch. Z., (2004), Controlled synthesis and self-assembly of single-crystalline copper oxide nanorods and nanoribbons. *Cryst. Growth. Des.* 4: 397-402.

[9] Yueming Li., Jing L., Zhanliang T., Jun Ch., (2008), Copper oxide particles and plates: Synthesis and gas-sensor application. *Mater. Res. Bull.* 43: 2380-2385.

[10] Jiang Z.-A., (2009), Copper oxide nanosheets synthesized by hydrothermal Process. *Chin. Phys. Lett.* 26: 0862021-0862023.

[11] Junwu Z., Huiping B., Yanping W., Xin W., Xujie Y., Lude L., (2007), Synthesis of flower-like copper oxide nanostructures via a simple hydrolysis route. *Mater. Lett.* 61: 5236-5238.

[12] Du G. H., Van Tendeloo G., (2004), Cu $(OH)_2$ nanowires, copper oxide nanowires and copper oxide nanobelts. *Chem. Phys. Lett.* 393: 64-69.

[13] Hafsa S. M. S., Qureshi F., Haque Z., (2016), Surfactant assisted wet chemical synthesis of copper oxide (Copper oxide) nanostructures and their spectroscopic analysis. *Optik.* 127: 2740-2747.

[14] Prakash Ch., Anurag G., Ashavani K., Umesh K. G., (2015), Effect of NaOH molar concentration on morphology, Optical and ferroelectric properties of hydrothermally grown CuO nanoplates. *Mater. Sci. Semicond. Process.* 38: 72-80.

[15] Allaedinia Gh., Aminayib P., Masrinda Tasirina S., Mahmoudi E., (2015), Chemical vapor deposition of methane In the presence of Cu/Si nanoparticles as a facile method for graphene production. *Fullerenes, Nanotubes and Carbon Nanostructures*. 23: 968-973.

[16] Liu J., Jun J., Zhao D., Shao-Zhuan H., Zhi-Yi H., Li W., Chao W., Li-Hua Ch., Yu L., Van Tendeloo G., Bao-Lian S., (2012), Tailoring CuO nanostructures for enhanced photo catalytic property. *J. Colloid and Interf. Sci.* 384: 1-9.

[17] Tanmaya B., Ranjan Kumar H., Sudhasu Sekhar N., Avinna M., Sahid A., (2014), Frequency and temperature dependence behaviour of impedance, modulus and conductivity of $BaBi_4Ti_4O_{15}$ Aurivillius ceramic. *Processing and Applic. Ceramics.* 8: 145-153.

[18] Priyanka Jha A. K., ( 2013), Electrical characterization of zirconium substituted barium titanate using complex impedance spectroscopy. *Bull. Mater. Sci.* 36: 135-141.

[19] Prakash Chandra S., Manisha A., Sunil Ch., Manoj K., Sandeep Ch., (2014), Structural, magnetic, vibrational and impedance properties of Pr and Ti co doped $BiFeO_3$ multiferroic ceramics. *Ceram. Int.* 40: 7805-7816.

[20] Suresh S., Priya M., (2015), Electrical properties of copper oxide nanoparticles. *J. Nano Res* 30: 1-8.

[21] Daries Bella R. S., Karthick prabhu S., Maheswaran A., Ambika C., Hirankumar G., Premanand D., (2015), Investigation of the Ionic conductivity and dielectric measurements of poly (N- Vinyl Pyrrolidone) - Sulfamic acid polymer complexes. *Physica B*. 458: 51-57.

[22] Deepthi K. R., Pandiyarajan T., Karthikeyan B., (2013), Vibrational, giant dielectric and AC conductivity properties of agglomerated Copper oxide nanostructures. *J. Mater. Sci: Mater Electron.* 24: 1045-1051.

[23] Elliott S. R., (1977), A theory of A.C. conduction in chalcogenide glasses. *Philosophical Magazine.* 36: 1291-1304.

[24] Karthickprabhu S., Hirankumar G., Maheswaran A., Daries Bella R. S., Sanjeeviraja C., (2014), Structural and electrical studies on $Zn^{2+}$ doped $LiCoPO_4$. *J. Electrostatics.* 72: 181-186.

[25] Suman C. K., Prasad K., Choudhary R. N. P., (2005), Impedance spectroscopic studies of ferroelectric $Pb_2Sb_3DyTi_5O_{18}$ ceramic. *Adv. Appl. Ceram.*104: 294-295.

[26] Sudipta S., Pradip Kumar J., Chaudhuri B. K., Sakata H., (2006), Copper (II) oxide as a giant dielectric material. *Appl. Phys. Lett.* 89: 2129051-2129053.